Environ Earth Sci (2011) 63:49–63
DOI 10.1007/s12665-010-0687-z

ORIGINAL ARTICLE

Comparison of the implementation of rock engineering system and analytic hierarchy process methods, upon landslide susceptibility mapping, using GIS: a case study from the Eastern Achaia County of Peloponnesus, Greece

D. Rozos · G. D. Bathrellos · H. D. Skillodimou

Received: 29 July 2009 / Accepted: 5 July 2010 / Published online: 1 August 2010

Abstract As landslides are very common in Greece, causing serious problems to the social and economic welfare of many communities, the implementation of a proper hazard analysis system will help the creation of a reliable susceptibility map. This will help local communities to define a safe land use and urban development. The purpose of this study is to compare the implementation of two semi-quantitative landslide assessment approaches, using landslide susceptibility maps compiled in a GIS environment. The compared methods are rock engineering system (RES) and the analytic hierarchy process (AHP). For the landslide susceptibility analysis, the Northeastern part of the Achaia County was examined. This area suffers from many landslides, because of its neighborhood with the tectonically active Corinthian Gulf and its geological setting (Neogene sediments, flysch and other bedrock formations, with local overthrusts). Ten parameters were used in both methodologies, and each one was separated into five categories ranging from 0 to 4, representing their specific conditions derived from the investigation of the landslides in the western part of the study area (ranking area). A layer map was generated for each parameter, using GIS, while the weighting coefficients of each methodology were used for the compilation of RES and AHP final maps of the eastern part of the study area (validating area). By examining these two maps, it is revealed that even though both correctly show the landslide status of the second site, the RES map reveals a better behavior in the spatial distribution of the various landslide susceptibility zones.

Keywords Rock engineering system · Analytical hierarchy process · GIS · Landslide susceptibility map · Peloponnesus · Greece

D. Rozos
School of Mining and Metallurgical Engineering, National Technical University of Athens, 9 Heroon Polytechniou str, 15780 Athens, Greece
e-mail: rozos@metal.ntua.gr

G. D. Bathrellos (✉) · H. D. Skillodimou
Department of Geography and Climatology, Faculty of Geology and Geoenvironment, National and Kapodistrian University of Athens, University Campus, Zografou, 15784 Athens, Greece
e-mail: gbathrellos@geol.uoa.gr

H. D. Skillodimou
e-mail: hskilodimou@geol.uoa.gr

Introduction

Landslides are among the most dangerous natural hazards worldwide affecting the development of an area. This is because they usually threat and influence the social and economic development of a community, apart from the very serious but not rare case of loss of human lives (Skidmore 2001). So, landslide hazard assessment is an important tool for the mitigation of this kind of disasters, but also a necessary step for land use and urban planning government policies worldwide (Carrara et al. 1991).

Therefore, the management of a landslide constitutes a very demanding condition for the protection of a human community. Unfortunately, in most cases, the action against the consequences of a landslide is restricted, like every other disaster, in the lower part of the disasters management cycle of Fig. 1 (Casale and Margottini 1999), and not in the upper one, which includes the prolepsis and other actions before the natural hazard manifestation. This fact reveals the lack of satisfactory field work and general planning of preparedness, at least in the case of the manifestation of many landslides, the prediction or mitigation

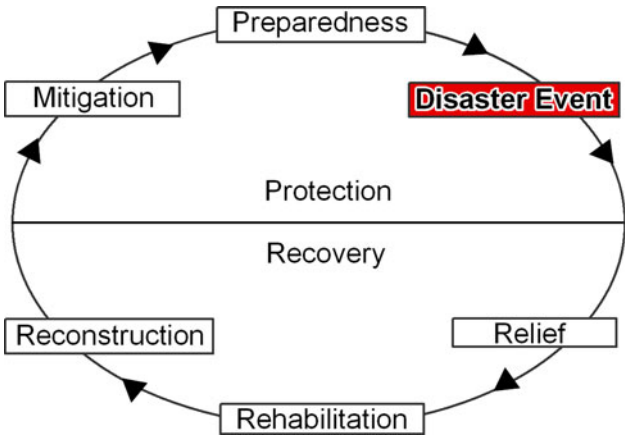

Fig. 1 The disaster management cycle (Casale and Margottini 1999)

of which is not dependant on multi various and unforeseen parameters, like seismic events.

During the recent decades, a lot of work has been done to the direction of prediction and mitigation of landslide phenomena, such as the use of landslide susceptibility and hazard maps especially for land use planning. The aim of these maps is to classify the various parts of land surface according to the degree of actual or potential landslide hazard. Thus, the final receivers of these products, namely, the local authorities will be able to manage better the sites for urban or industrial planning and development.

The reliability of these maps depends mostly on the applied methodology as well as on the available data used for the hazard risk estimation (Parise 2001). To this direction, GIS can help a lot with the spatial analysis of a landslide, i.e., a multi-dimensional phenomenon. Moreover, GIS is an excellent and useful tool for mapping the susceptibility of an area prone to landslide manifestation (Van Westen et al. 1999; Saha et al. 2002; Chau et al. 2004; Lan et al. 2004; Yilmaz 2009a).

On the other hand, the semi-quantitative landslide assessment approaches (methods), like RES or AHP, can be considered as an effective expert's tool for weighting and ranking the chosen parameters in an objectively optimal and simple way, which represent the main causes for landslide susceptibility of the study area.

The rock engineering system (RES), a multi-objective system, has been established and developed by J.A. Hudson, as a response to the need for a semi-quantitative technique to approach increasingly complex rock engineering problems. The approach is an objective-based methodology, which is capable of utilizing all the relevant information to a particular project (Hudson 1992). The implementation of this methodology is achieved through an interaction matrix, which is considered to be the basic tool, and a valuable technique for simultaneous representation of the selected parameters and the coded expressions of all binary interactions ranking from zero to four. The selected parameters are shown in the main diagonal cells of the matrix, while the rankings are presented in off-diagonal cells, expressed in properly coded form. This methodology has already been successfully applied on rock mass characterization engaged in the assessment of natural slope instability (Mazzoccola and Hudson 1996) but also on ranking the landslide potential of slopes with various geological formations (Rozos et al. 2006, 2008).

The analytical hierarchy process (AHP) is also a semi-quantitative, multi-objective and multi-criteria decision-making methodology (Saaty 1990, 2006), which has been widely applied for the solution of decision problems. This method comprises the analytical hierarchy of involved parameters and the comparison between the various pairs of them for the assignment of a relevant ratio for each parameter. In other words, it can estimate the weight of each parameter according to their preference, through the linear correlation of each one relative to the others. This is achieved by means of relevant correlation of them in pairs, as they are shown in a relative matrix, regarding the landslide vulnerability of the area. The ability of correlating different parameters, made this method a valuable tool for many researchers in compiling landslide susceptibility maps (Ayalew et al. 2004, 2005; Komac 2006; Yoshimatsu and Abe 2006; Castellanos Abella and Van Westen 2007; Yalcin and Bulut 2007; Akgün and Bulut 2007; Akgün et al. 2008).

Because the above two methodologies involve the handling and linear correlation of a large amount of factual and simulated data, the geographical information system (GIS) was employed for the success of such an analysis, as many other researchers have made, in calculating and managing natural hazards (Carrara et al. 1991). In this study, both methods (RES and AHP) were adopted in a GIS environment for the compilation of the corresponding landslide susceptibility maps. Regarding the correlation ascribed by each methodology, these final maps give useful information of the causal parameters and the landslide manifestation in the study area. Therefore, the relevant comparison of the maps reveals the benefits and deficits of one method in relation to the other.

Study area

Location and geomorphologic framework

The study area is part of Achaia County, which is located in the Northeastern part of Peloponnesus and considered as one of the most mountainous regions of Greece, since 60% of its total area is highland (up to 2,341 m). The study area has an expanse of about 420 km^2 and its altitude varies from 0 to 1,760 m (Fig. 2). The landscape evolution of this

area is controlled by the neotectonic action of the graben, which forms the Corinthian gulf. Therefore, the drainage network is well developed (Fig. 2), as it is controlled by fault tectonics in many cases, with its main axes to be orientated from SW to NE, namely the conjugate direction of the graben margin faults (Fig. 3).

With regard to the climatic conditions of the study area (NE Peloponnesus), the precipitation varies from 550–970 mm and because of its coastal extension the climate is classified as mild Mediterranean, without considerable temperature variations (Helias 1978). The generally wet winter and dry summer are the defining characteristics of this climate.

Geological structure and tectonics

Formations from three Hellenic geotectonic zones (Olonos–Pindos, Gavrovo–Tripolis and Ionian) participate in the geological structure of Achaia County. Also, the existence of Corinthian graben with recent geodynamic evolution in its immediate vicinity, results in an increased seismic activity. Therefore, Achaia is characterized by a complicated geological structure with prevailing tectonic fracturing, as Pindos zone constitutes an extended overthrusted cup on Gavrovo zone formations (Rozos 1989). Furthermore, this intense tectonic activity has brought about the formation of successive tectonic napes, mainly in the frontal part of the overthrust, which characterize the Pindos zone. The neotectonic action influences the development of the Plio-Pleistocene sediments of the County, which are mainly lacustrine to marine–lacustrine deposits. The total thickness of these sediments ranges from 350 to 2,000 m, explaining the great uplifting movements taking place in the referred region.

This geotectonic evolution is also reflected in the study area, where the bedrock consists of formations only from the Olonos–Pindos geotectonic zone with the above referred "inherent weaknesses" that are connected with the alpine

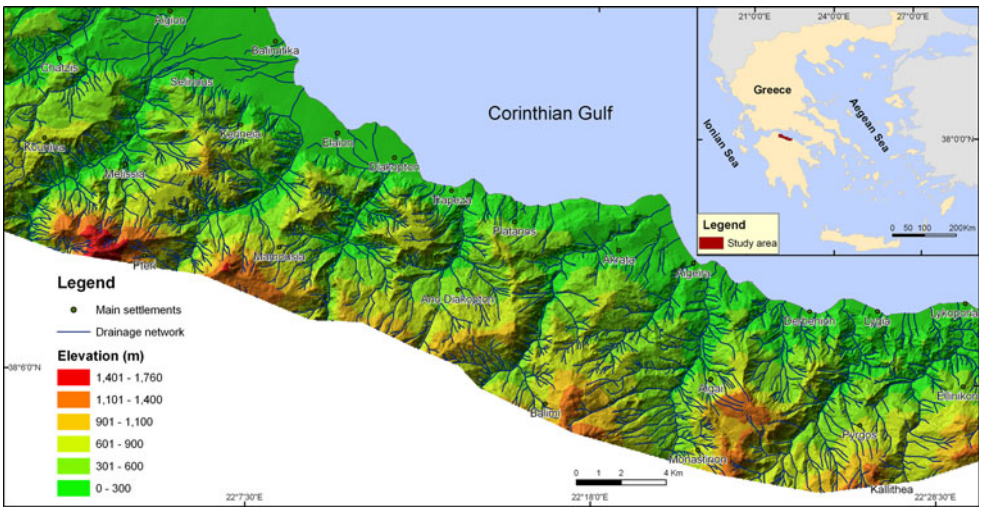

Fig. 2 The location map of the study area, with classes of elevation and drainage network

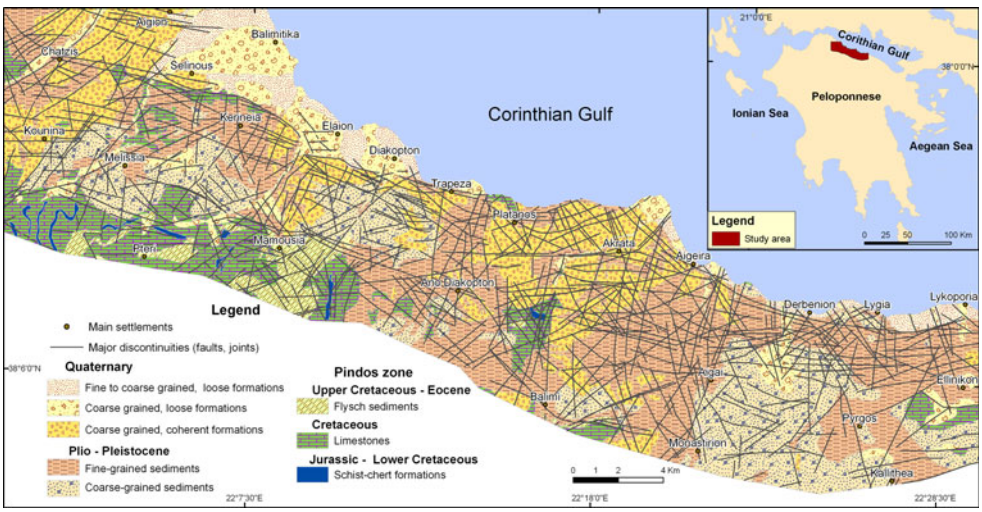

Fig. 3 The simplified geological map of the study area

cycle of sedimentation and orogenesis (Tsoflias 1970). Moreover, the induced stresses due to neotectonic movements must be considered in that area, which is a part of the still active Corinthian graben (Doutsos et al. 1987, 1988; Papanastassiou et al. 1993; Gaki-Papanastassiou et al. 1996). Therefore, the formations of that area and mainly the Plio-Pleistocene sediments exhibit a great instability due to their active tectonism, lithology, high seismicity, their abrupt morphology as well as the human activity.

As presented in the simplified geological map in Fig. 3, the study area is composed of (Rozos 1989; Koukis and Rozos 1982):

a. Fine-grained to coarse-grained loose Quaternary formations consisting of clays, silts, siltstones and sands of a fluvial–lacustrine, lagoon, and/or Aeolian origin as well as weathering products of older formations. Also, loose deposits of mixed phases, such as clayey silts, siltstones, sands of a ranging grain size distribution, and grits are also present.
b. Coarse-grained loose Quaternary formations. Clastic formations mainly of pebbles and gravels of varying sizes with a minimum proportion of fine-grained materials, screes and fans.
c. Coarse-grained coherent Quaternary formations. They are polygenic conglomerates, usually poorly graded and/or slope breccias, but also semi-cohesive conglomerates, sands with a low degree of diagenesis and rocky fragments with red clay as a cementing material participate. All Quaternary deposits present a quick alteration of phases, both vertically and horizontally.
d. Fine-grained Plio-Pleistocene sediments with a variety of lithological horizons. They consist of clays, marls, alternating sands of a varying degree of diagenesis and/or their mixed phases.
e. Coarse-grained Plio-Pleistocene sediments consisting of conglomerates, usually strongly cemented, with pebbles and clayey-sandy cementing material.
   In general Plio-Pleistocene sediments can be subdivided into two main horizons: the lower one, which includes fine-grained facies (alternations of clayey marls, marls, silty sands and weak sandstones), and the upper one that resulted from a progressive transition of the sediments upwards to the coarser facies, giving finally coherent conglomerates of a great thickness.
f. Flysch formations of Central Greece. Their main members are sandstones, siltstones and more rarely conglomerates. They are Cyclothematic and strongly folded sediments because of the tectonic action (nappes and upthrusts), which in many places results in the formation of thick weathering mantle.
g. Carbonate rocks. They consist of Cretaceous limestones of Central Greece, which usually are moderate to thick-bedded limestones, folded and karstified, with thin intercalations or nodules of silica lumps, but also with rare intercalations of claystones or siltstones.
h. Schist–chert formations. Alternations of cherts, siltstones, thin-plated limestones and sandstones while volcanic tuffs rarely participate at places. Thick weathering mantle is formed, mainly in the cases of the surface occurrence of siltstones.

Regarding the faults and major discontinuities encountered in the area, the examination of air photos and the field work revealed that their distribution and orientation show a great dispersion, with domination of N70°–90°E, N30°–40°W, N40°–50°E, N70°–80°W and N10°–20°E sets. The two-first (N70°–90°E, N30°–40°W) are the oldest ones and resulted from the general uplifting of the area, while the rest are connected with the migration of the Aegean arch (Doutsos et al. 1988).

Data and methodology

The following sources and data were used employing GIS, in preparing the two landslide susceptibility maps for the comparison of RES and AHP:

a. Topographic maps of Greek Military Service at a scale of 1:50,000,
b. The geological map of Greece at a scale of 1:50,000, Sheets Aigion and Dervenion of Institute of Geology and Mineral Exploration, IGME (1993, 2005).
c. The engineering geological maps of Achaia County at a scale of 1:50,000 and 1:100,000 (Rozos 1989),
d. Precipitation records from eight stations, belonging to: (1) the Hellenic National Meteorological Service, (2) the Ministry for the Environment, Physical Planning and Public Works, (3) the Ministry of Agriculture and Ministry of Development. These records referred to mean annual precipitation for the period of 1975–2007.
e. The fieldwork of this study carried out during 2008–2009.

All the available data were utilized in the effort of the selection of the principal parameters and then for their GIS thematic layers. More analytically, the GIS software ArcGIS v.9.3 was used for the creation of every data layer map. These maps were elaborated for the compilation of the final landslide susceptibility maps. At the beginning, all the relevant topographic, geological, tectonic and landslide manifestation maps were digitized. In the next step, the data from the topographic maps were used for the generation of the digital elevation model (DEM), with a cell size of 60 × 60 m, which was utilized in this study for the generation of the grid maps.

Adopting the methodology, which processes and analyses data in one part of the study area and validates them in another (Remondo et al. 2003; Irigaray et al. 1999, 2007), the study area was subdivided into two parts, following the boundaries of the two topographic maps involved. The western part, called Aigion area, was chosen to be the ranking site, where the characteristics of the slope movements, the experience of the study team, and the suggestions of previous works helped in the selection of the principal parameters. The weighting coefficients of these parameters were selected and applied in both methods. The Eastern part, called Dervenion area, was the validating site. The manifested landslides of this site were used for the application and validation of RES and AHP methods, and their final landslide susceptibility maps were compiled. The comparison of these two maps led to the final conclusions regarding the validity of each method.

Landslide inventory map

The landslides, recorded from previous works (Rozos 1989), but also those recorded during the fieldwork of this study, were used for the compilation of the landslide manifestation map both in ranking and validating area (Fig. 4). The main scarp of every recorded landslide during the field work was depicted in topographic maps at a proper scale and then was digitized as polygon layer. According to Yilmaz (2009b) the scarp sampling strategy gives better results than the point one. A number of 547 sites of landslide manifestation were examined throughout the study area, having affected a mean area up to 91,000 m^2. From these sites, 277 are the landslides affected the ranking area and were used for establishing the principal parameters, their ratings and their weighting coefficients for both methods, while the rest (270) are the landslides manifested in the validating area, i.e., the landslides used for the comparison of the implementation of the two methods.

The parameters involved and their rating

The selection of the appropriate parameters has been based on: (a) valuable knowledge from the work of other researchers, where similar methodologies have successfully been applied (Larsen and Parks 1997; Glade1998; Guzzetti et al. 1999; Donati and Turrini 2002; Guthrie and Evans 2004; Ayalew and Yamagishi 2005; Moreiras 2005; Jurko et al. 2005; Kanungo et al. 2006; Lee and Sambath 2006; Rozos et al. 2006; Lee and Pradhan 2007; Rozos et al. 2008; Bathrellos et al. 2009); (b) the overall knowledge gained from the study of landslide phenomena in Greek territory (Koukis and Rozos 1982; Koukis 1988; Koukis and Sabatakakis 2000); (c) the experience gained through the systematic investigation and study of landslide activity in Achaia County (Koukis et al. 1997; Rozos 1989); and (d) the extended field observations in the frame of this study.

The parameters which were finally selected for the two applied methodologies were the following ten: (1) lithology, (2) distance from tectonic lineaments, (3) slope angle, (4) slope aspect, (5) rainfall, (6) altitude, (7) land use, (8) distance from roads, (9) distance from rivers, and (10) geometry of main discontinuities.

Each parameter was then separated into 5 classes, with a rating from 0 to 4 according to restrictions of RES method. Every class represents specific conditions, as they have been investigated and recorded in the study ranking area. Thus, the class, which was rated as 0, represented the most stable conditions (minor landslide risk) and the one rated as 4 the most favorable conditions for slope failure (major landslide risk). In Table 1 the selected principal parameters, their classes and their ratings are shown, alongside the relative density of the landslides. The density of landslides

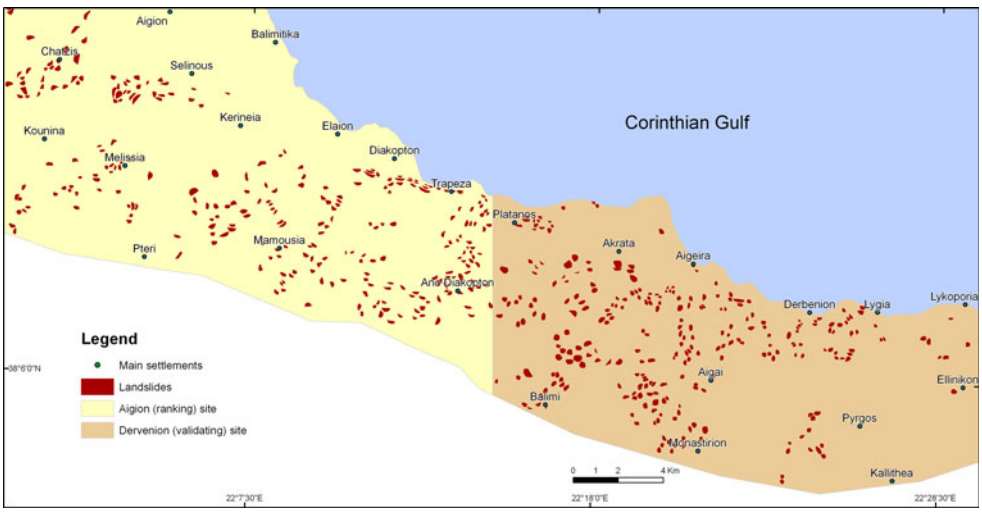

Fig. 4 Map showing the landslide distribution in the separated two parts of the study area. The Aigion (ranking) site and the Dervenion (validating) site

is the ratio between the areas covered by the pixels of landslides, which represent a class of a parameter and the total landslide area. This density, expressed in percentages, was thought to be the basic factor for the rating of every class of the principal parameters.

Lithology

Lithology is one of the most decisive parameters regarding the landslide manifestation. For the study area the classes of lithology have arisen from its geological setting, based on literature (IGME 1993, 2005; Rozos 1989) and fieldwork. The distinctive geological formations were digitized and unified according to their engineering geological behaviour, in relation to landslide manifestation. Thus, lithology includes five classes as follows: (a) moderate to thick-bedded limestones, (b) thin bedded schist chert formations, (c) Plio-Pleistocene coarse-grained sediments, (d) fine, fine-coarse to coarse and loose to semi-coherent Quaternary formations, (e) Cyclothematic formations (Plio-Pleistocene fine-grained sediments and Flysch sediments).

Regarding the density of landslides, the higher percentage is attributed to Cyclothematic formations (Plio-Pleistocene fine-grained sediments and Flysch formations) and thus this class has the higher rate (4).

Table 1 Classes and ratings of adopted principal parameters, with landslide density (%) distribution for each class

Description	Landslide density (%)	Rating	Description	Landslide density (%)	Rating	Description	Landslide density (%)	Rating
1. *Lithology*			2. *Distance from Tectonic lineaments*			3. *Slope angle*		
Moderately to thick-bedded limestones	2.36	0	Distant (>200 m)	11.13	0	0–5°	13.63	0
Thin bedded schist chert formations	3.15	1	Moderate distant (151–200 m)	8.30	1	6°–15°	20.63	1
Plio-Pleistocene coarse-grained sediments	16.65	2	Near (101–150 m)	14.18	2	16°–30°	42.10	2
Quaternary formations fine, fine –coarse to coarse, and loose to semi-coherent	23.32	3	Very near (51–100 m)	27.78	3	31°–45°	17.97	3
Plio-Pleistocene fine-grained sediments and Flysch formations	54.52	4	Nearest (0–50 m)	38.60	4	>45°	5.67	4
4. *Slope aspect*			5. *Rainfall*			6. *Altitude*		
181°–225°	9.89	0	<650 mm	0.00	0	>1,200 m	0.00	0
136°–180°	10.01	1	650–700 mm	2.90	1	801–1,200 m	5.57	1
91°–135°, 226°–270°	23.52	2	701–750 mm	14.29	2	501–800 m	20.27	2
46°–90°, 271°–315°	25.69	3	751–800 mm	27.98	3	<250 m	29.15	3
0°–45°, 316°–360°	30.88	4	>800 mm	54.83	4	250–500 m	45.01	4
7. *Land use*			8. *Distance from roads*			9. *Distance from rivers*		
Barren areas	1.20	0	Distant (>200 m)	17.01	0	Distant (>200 m)	18.54	0
Urban areas	4.44	1	Moderate distant (151–200 m)	8.09	1	Moderate distant (151–200 m)	12.13	1
Forest areas	13.70	2	Near (101–150 m)	14.50	2	Near (101–150 m)	14.08	2
Shrubby areas – Natural grasslands	37.95	3	Very near (51–100 m)	24.42	3	Very near (51–100 m)	22.85	3
Cultivated areas	42.71	4	Nearest (0–50 m)	35.98	4	Nearest (0–50 m)	32.4	4
10. *Geometry of main discontinuities*								
Drive against	23.07	0						
Drive sideways and vertical	23.79	1						
Drive with, having a dip of >30°	10.9	2						
Drive with, having a dip of 1–15	18.34	3						
Drive with, having a dip 16–30°	23.9	4						

Distance from tectonic lineaments

The active tectonics in the study area plays an important role in the landslide manifestation. The various tectonic lineaments were collected from literature (IGME 1993, 2005; Rozos 1989) and fieldwork. All tectonic lineaments (faults, overthrusts, etc.) were digitized and buffer zones were formulated around them at distances of 50, 100, 150 and 200 m. Thus, the classes of the buffer zones are five, namely: (1) the nearest (0–50 m), (2) the very near (51–100 m), (3) the near (101–150 m), (4) the moderate distant (151–200 m) and (5) the distant (>200 m). As it was expected the lower the landslide density values the higher the distance from the relevant tectonic lineaments. Thus, the most prone class to landslide is that of 0–50 m, taking the highest rate (4).

Slope angle

The angle and the aspect of the slopes play a very important role in the manifestation of the landslides because they express the result of the combined influence of many agents (Rozos et al. 2008). Contours with 20 m intervals were digitized from topographic sheets and saved as line layer. A digital elevation model (DEM) was derived from the digitized elevation data using 3D analyst extension of ArcGIS, and the slope layer was extracted from it. The grid maps of the slope angle with cell size 60 × 60 m were classified into five classes, as follows: (1) 0°–5°, (2) 6°–15°, (3) 16°–30°, (4) 31°–45°, and (5) >45°, with the higher rating to be given to the slopes with the higher inclination, despite the higher landslide density is in the classes 6°–15° and 16°–30°. This peculiar condition can be explained easily as in nature, slopes consisting of soil or hard soil to soft rocky formations (like those of the study area), and having high angle, fail almost immediately after their formation giving lower slope angles. Finally, the slopes with an inclination of around the angle of friction are those, which fail after the action of triggering factors. On the other hand, rocky slopes are stable even in high angles suffering only from rock falls, wedge failures, etc.

Slope aspect

For the classification of the slope aspect, the grid maps of this parameter were produced with cell size 60 × 60 m elaborating the DEM. These maps were classified into five classes, including in some cases more than one range of aspects, namely: (1) SW 181°–225°, (2) SE 136°–180°, (3) ESE 91°–135° and SWW 226°–270°, (4) NEE 46°–90° and WNW 271°–315°, (5) NNE 0°–45° and NWN 316°–360°. As it was revealed from the fieldwork, most of the landslides are manifested in the slopes with orientation from northwest to northeast. So these orientations constitute the classes with the higher rating 3 and 4 (Table 1).

Rainfall

As it is well known, precipitation is among the most usual triggering factors for landslide manifestation. The stations used are well distributed in the study area both hypsometrically and territorially, giving very good results regarding the distribution of the precipitation. The mean annual precipitation of the area is between 550.7 and 973.1 mm. For the necessities of this study, the precipitation map was produced, using the data of the main meteorological stations in the area and applying the Inverse distance weighted (IDW) interpolation method. This map was separated into 5 classes, i.e.: (1) <650 mm, (2) 651–700 mm, (3) 701–750 mm, (4) 751–800 mm, and (5) >800 mm. Landslide density percentage is higher as the precipitation increases and thus the higher the precipitation, the higher the rating (Table 1).

Altitude

The altitude does not contribute directly to landslide manifestation, but in relation to the other parameters, like tectonics, erosion–weathering processes, and precipitation, the altitude contributes to landslide manifestation and influences the whole system (Rozos et al. 2008). The grid maps of the altitude with cell size 60 × 60 m were produced from the DEM. The separation of the altitude into 5 classes, i.e. (1) <250 m a.s.l., (2) 250–500 m a.s.l., (3) 501–800 m a.s.l., (4) 801–1,200 m a.s.l., and (5) >1,200 m a.s.l., was based on the morphology of the study area in relation to the landslide occurrence. The increasing of the altitude is not in a direct relation to the landslide density, with the higher density percentage to attributing to second class (250–500 m a.s.l.). This is because Plio-Pleistocene sediments with the maximum percentage of landslide density mainly occupy the hilly to semi-hilly morphological relief (Table 1).

Land use

The data for the land use were taken from CORINE program (Bossard et al. 2000) and were saved as polygon layer. The variation of the vegetation in an area is a parameter that seriously affects the slope failures, as slope stability is very sensitive in changes on vegetation. For the necessities of this study, the land use, which reflects the vegetation covering, was classified into 5 categories as follows: (1) barren areas, (2) urban areas, (3) forest areas, (4) shrubby areas–natural grasslands, and (5) cultivated areas. The maximum percentage of landslide density is

attributed to cultivated areas with the higher rating (Table 1).

Distance from roads

As it is obvious, the artificial and natural parts of the slopes around a road are more sensitive in landslide manifestation. Therefore, the road network was chosen as a principal parameter and was digitized and saved as line layers in the GIS database, using the topographic sheets as data source. Buffer zones were created around the roads of the area at distances of 50, 100, 150 and 200 m. Thus, the classes of the buffer zones are five, namely: (1) the nearest (0–50 m), (2) the very near (51–100 m), (3) the near (101–150 m), (4) the moderate distant (151–200 m) and (5) the distant (>200 m). The highest percentage of landslide density refers to the "nearest" class with the high rating (Table 1).

Distance from rivers

Similar to the road network, the hydrographic network was digitized and saved as line layers in the GIS database, using the topographic sheets as data source. The hydrographic axes continuously change the slopes of the rivers and can therefore be considered as one of the principal parameters in landslide manifestation. For the examination of this parameter, buffer zones were created around the bed of the rivers and the streams of the area, at distances of 50, 100, 150 and 200 m. These distances start counting from the river's bed boundaries from both sides. This is because the beds of the rivers are usually flat places where no landslide occurs. Finally, the classes of the buffer zones are also five, like for roads: (1) the nearest (0–50 m), (2) the very near (51–100 m), (3) the near (101–150 m), (4) the moderate distant (151–200 m) and (5) the distant (>200 m). The percentage of landslide density reduces as the distance from the hydrographic axes increases, thus, the highest percentage of landslide density refers to the nearest class (Table 1).

It is noticeable that in roads and rivers, but also in tectonic lineaments a significant percentage of landslide density is ascribed to distances >200 m. This is not peculiar, as other parameters affect the area >200 m and influence the landslide manifestation.

Geometry of main discontinuities

The geometry of the main discontinuities in relation to slope geometry (aspect) is strongly related to the stability of hard soils, and soft rocks. Thus, the map of the main discontinuities was compiled using the relevant literature (Rozos 1989; IGME 1993, 2005) and the observations during the fieldwork. The recorded dips and dip directions of the formations were digitized and saved as a map of GIS database. The formations without dip were characterized as "no data formations". In a next step, the map was converted in raster format and combined to the slope aspect map. Therefore, the correlation of the dip direction of strata with the slope aspect was able to be done and the classes "drive against", "drive sideways and vertical" as well as "drive with" were formulated, with the highest percentage of landslide density to be attributed to the "drive with" class. With regard the "drive with" class, its combination with the friction angle of the Cyclothematic formations (Neogene and flysch) gave space in another three classes namely "drive with having a dip of 1°–15°", "drive with having a dip 16°–30°" and "drive with having a dip of >30°". Thus, the overall classes were 5, as follows: (1) drive against, (2) drive sideways and vertical, (3) drive with, having a dip of 1°–15°, (4) drive with, having a dip 16°–30°, (5) drive with, having a dip of >30°.

The thematic layers of the ten principal parameters involved in this study are given in Fig. 5. After selecting and rating the principal parameters, the main consideration was to build the interaction matrix for both methods, which will help in finding the weighted coefficients of each parameter.

The utilized methods

RES method

The interaction matrix, as presented below (Table 2), shows in its main diagonal cells the principal parameters which are considered responsible for controlling the potential instability of natural slopes and in its off-diagonal cells the coded expressions of all possible binary interactions, according to the judgment of the people involved in this study. Therefore, referring to the matrix coding, a semi-quantitative approach based on experts judgment was used, ranging from zero to four, corresponding to no, weak, medium, strong and critical interactions, respectively. The influence of each parameter on the system (named cause, C) and the influence of the system on each parameter (named effect, E) are presented in an external row and column, respectively.

The role of each parameter in slope failure, i.e., the interactive intensity $(C + E)$, and finally the weighted coefficient (W_i) in a percentage form $\left\{\frac{1}{4}\frac{(C+E)}{\left(\sum_i C+\sum_i E\right)}0/0\right\}$, which influences the system, is given in Table 3. These weighting coefficients express the proportional share of each parameter as a failure-causing parameter in slope failure.

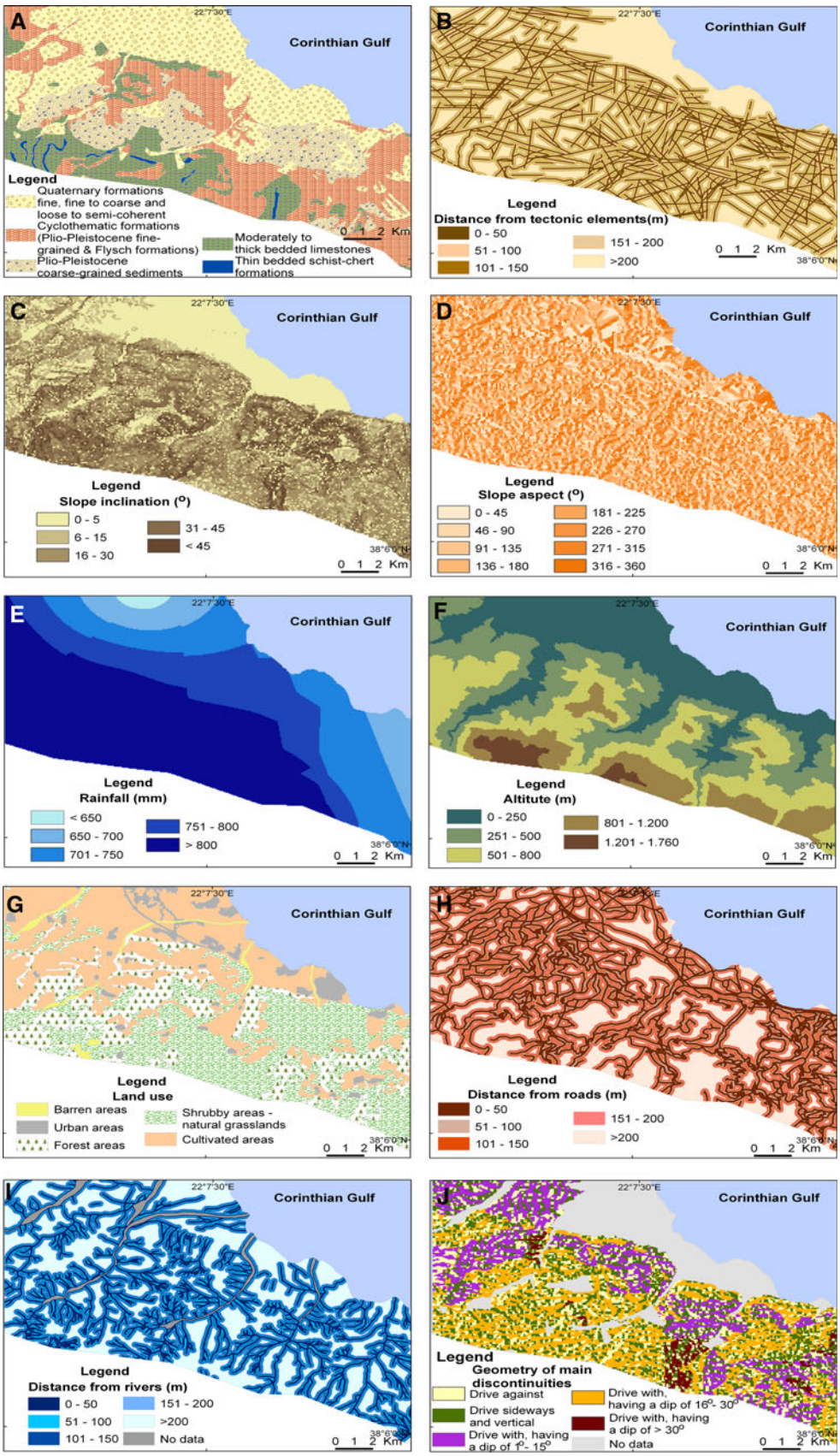

Fig. 5 The thematic layers of the ten principal parameters involved in this study. **a** Lithology, **b** distance from tectonic lineaments, **c** slope angle, **d** slope aspect, **e** rainfall, **f** altitude, **g** land use, **h** distance from roads, **i** distance from rivers, **j** geometry of main discontinuities

Table 2 The interaction matrix of the RES method

INTERACTION MATRIX												
P1	2	3	3	0	2	4	1	2	2	3	22	CAUSE – C
0	**P2**	3	1	0	1	0	2	3	2	3	15	
1	2	**P3**	1	0	0	4	3	2	2	4	19	
0	0	2	**P4**	1	0	2	1	1	1	3	11	
2	2	3	0	**P5**	0	1	3	3	1	4	19	
1	1	2	0	4	**P6**	3	2	1	0	1	15	
0	1	0	0	0	1	**P7**	1	1	1	3	8	
0	1	0	1	1	0	0	**P8**	0	1	3	7	
1	1	0	2	3	0	2	0	**P9**	1	3	13	
1	3	3	3	1	1	2	3	3	**P10**	3	23	
0	0	0	0	0	0	0	0	0	0	**P11**	0	
6	13	16	11	10	5	18	16	16	11	30	152	
EFFECT - E												

P1 = LITHOLOGY	P2 = DISTANCE FROM TECTONIC	P3 = SLOPE	P4 = SLOPE ASPECT
P5 = RAINFALL	P6 = ALTITUDE	P7 = LANDUSE	P8 = DISTANCE FROM ROADS
P9 = DISTANCE FROM RIVERS	P10 = GEOMETRY OF MAIN DISCONTINUITIES		P11 = POTENTIAL INSTABILITY

Table 3 The principal parameters, their interactive intensity and their weighting coefficient for the RES method

	Parameters	$C + E$	$\frac{(C+E)}{(\sum_i C+\sum_i E)}\%$	P_{ij}	Weighting coefficient (W_i)
1	Lithology	28	10.22	4	2.56
2	Distance from tectonic lineaments	28	10.22	4	2.55
3	Slope angle	35	12.78	4	3.19
4	Slope aspect	22	8.03	4	2.01
5	Rainfall	29	10.58	4	2.65
6	Altitude	20	7.30	4	1.82
7	Land use	26	9.49	4	2.37
8	Distance from roads	23	8.39	4	2.10
9	Distance from rivers	29	10.8	4	2.65
10	Geometry of main discontinuities	34	12.1	4	3.0
Total		274	100.00		25.00

From the above Tables 2 and 3, it is obvious that the most interactive parameter is the slope angle ($W_i = 3.19$), while the less interactive is the altitude ($W_i = 1.82$). Also, the lithology with the highest Cause number (22) is the parameter, which dominates the system and the distance from the roads with the lowest Cause number (7) is dominated by the system (Mazzoccola and Hudson 1996; Rozos et al. 2008).

AHP method

The AHP method is well known and widely used for the solution of multi-parametric problems, as the factors for the landslide susceptibility maps can be evaluated by it. The application of this method implements a linear correlation of the parameters involved, while their weighting coefficients are revealed via pair-wise comparison from a table-matrix with the relevant values. The pair-wise comparison process is performed using a nine point scale, the numerical values of which and the corresponding levels of importance are: 1 = equal, 3 = moderately, 5 = strongly, 7 = very strongly, 9 = extremely 2,4,6,8 = intermediate values (Saaty 1977).

During the construction of the table-matrix every principal parameter is rated in relation to any other with a value from 1/9 to 9. These numerical values represent the relevant significance of a parameter to the others regarding its applicability for the purpose of the study.

When the comparison is applied vice versa, the adopted numerical value is the reciprocal of the first one. In a next

step, all the numerical values are normalized by dividing each entry of every column by the sum of all the entries in that column, so that they sum up to 1. Following the subsequent normalization, the values were averaged across the rows to give the relative importance weight for each factor (Saaty 2006).

The calculation of the weighting coefficient of every adopted principal parameter in this study for AHP method is given in Table 4. After the creation of the table-matrix and the correlation of the principal parameters, its implication was checked with consistency ratio (CR). This ratio is used in order to avoid the creation of any incidental judgment in the matrix. According to Saaty (1990) when the consistency ratio is less than 0.1, the calculated weighting coefficients are acceptable. On the contrary, if that ratio is greater than 0.1, then, a reassessment of the judgments is demanded in the table-matrix. The CR from the application of the AHP in this study is 0.05 (Table 4). Thus, the judgments depicted in Table 4 are well assessed. All the pair comparisons, the eigenvectors, the weights and the consistency ratio were calculated using the Expert Choice 11 software.

Finally, as it can be seen from Table 4 the parameter with the highest weighting coefficient is the inclination of the slopes, followed by the rainfall, the geometry of main discontinuities and the lithology.

Results

After the application of the RES and AHP, a linear correlation between the weighting coefficients of both methods and the raster layers of the principal parameters involved was established, aiming to the total estimation of the ratings. Thus, the compilation of the final two landslide susceptibility maps was feasible. This linear correlation is given by the formula:

$$O = \sum_{i=1}^{n} P_i W_i$$

where, O = the overall score, n = the number of the parameters, P_i = the parameter i, W_i = the weighting coefficient of the parameter i.

Landslide susceptibility maps

After the interaction of the examined principal parameters for both methods and the calculation of their weighting coefficients (Tables 3, 4), these coefficients were linearly correlated with the relevant thematic levels. This procedure helps in the compilation of the final susceptibility maps, the comparison of which allows the final estimation on the possible predominance of one method to the other.

For the conversion of the maps into one or more categories with the continuous data technique, various classifier systems exist such as natural breaks, quantiles, equal intervals, standard deviation, etc. Ayalew et al. (2004), discussing the use of the above systems in the assortment of landslide susceptibility maps, concluded that the most suitable is the standard deviation. Therefore, the classification at present was carried out using standard deviation and the examined area was separated into five categories of landslide susceptibility, as follows: (1) very low, (2) low, (3) medium, (4) high and (5) very high. The compiled susceptibility maps from RES and from AHP are given in the Figs. 6 and 7, respectively.

Table 4 The principal parameters and the calculation of their weighting coefficient for the AHP method

	P1	P2	P3	P4	P5	P6	P7	P8	P9	P10	Weighting coefficient, W_i
P1	1	2	1/3	3	1/2	7	3	2	3	1	0.123
P2		1	1/3	2	1/2	6	2	1	1	1/2	0.072
P3			1	5	2	9	5	3	4	3	0.249
P4				1	1/5	6	1/2	1/4	1/5	1/6	0.033
P5					1	7	4	3	2	2	0.167
P6						1	1/5	1/8	1/8	1/7	0.014
P7							1	1/3	1/3	1/6	0.040
P8								1	1/2	1/2	0.077
P9									1	1/2	0.091
P10										1	0.135

P1 =LITHOLOGY	P2 = DISTANCE FROM TECTONIC	P3 = SLOPE	P4 = ASPECT
P5 = RAINFALL	P6 = ALTITUDE	P7 = LAND USE	P8 = DISTANCE FROM ROADS
P9 = DISTANCE FROM RIVERS	P10 = GEOMETRY OF MAIN DISCONTINUITIES	CR=0.05	

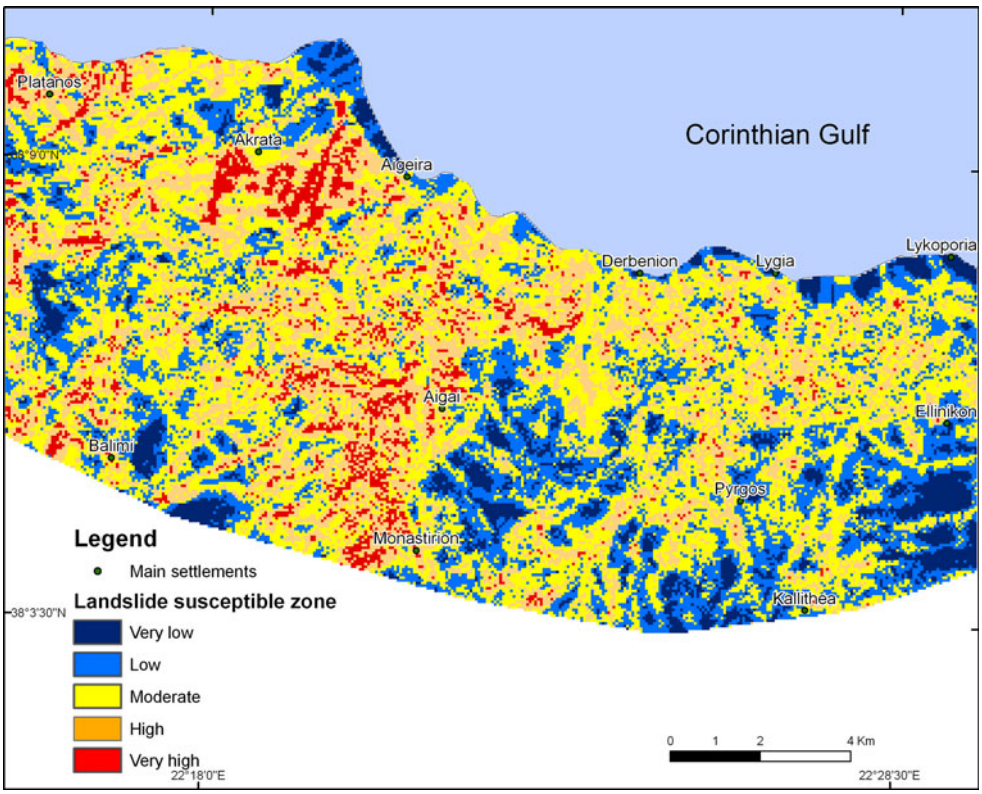

Fig. 6 The landslide susceptibility map from the RES method

Discussion on comparisons and validation of the produced maps

Discussing the appearance of the two compiled maps, it is revealed that the spatial distribution of the landslide susceptibility zones is the same in both methods applied, with the very high zone to have its largest distribution in the western part of validation area. Furthermore, examining the differences in the spatial distribution of two methods, the largest concentration of the very high susceptibility zone in the northwestern part of the map from RES method should be stressed (Fig. 6). On the contrary, the dispersion of the high susceptibility zone is noticeable in the same part of AHP map (Fig. 7). In reality, the northwestern part of validating area suffers from a large number of landslides because of the geological and morphological conditions prevailing there. Indeed this area is a hilly one with rather steep slopes and consists of Plio-Pleistocene sediments, prone to landslide manifestation.

Regarding the spatial development of the landslide susceptibility zones, their percentages to the total area from RES map are: 7.41% for the "very low" zone, 22.61% for the "low" zone, 38.59% for the "medium" zone, 25.00% for the "high" zone and 6.39% for the "very high" zone. The relevant percentages for AHP map are: 6.97% for the "very low" zone, 23.60% for the "low" zone, 38.16% for the "medium" zone, 24.75% for the "high" zone, 6.52% for the "very high" zone. These records reveal that the map of the RES method shows lower percentages for low and very high zones, while those for very low, moderate, and high susceptibility zones are higher, in relation to the corresponding zones from AHP map, but without any meaningful deviation.

Looking at the validity of each method, the two landslide susceptibility maps including the landslides manifested in Dervenion site were compared, and the density percentages of the landslides that fall into every zone of landslide susceptibility, were calculated. The results are given in Table 5.

As it is obvious from the above table, RES method gives better results in every zone. It depicts higher percentages for the "very high" and "high" zones and smaller for the "medium", "low" and "very low" susceptibility zones.

Also, as the very high and high susceptibility zones are of high importance in the land use and urban development of an area, it is valuable to correlate the landslide percentages, which fall into these zones, with the respective areas. This correlation was done by means of an index, which is called Landslide Models Indicator (LaMI) and comes from the division of landslide percentages in every susceptibility zone to respective area percentage (Bathrellos et al. 2009). The highest LaMI value coming up for a specific susceptibility zone, the more reliable are the results derived. The results of this comparison for very high and high susceptibility zones are given in Table 6, revealing the better applicability of the RES method.

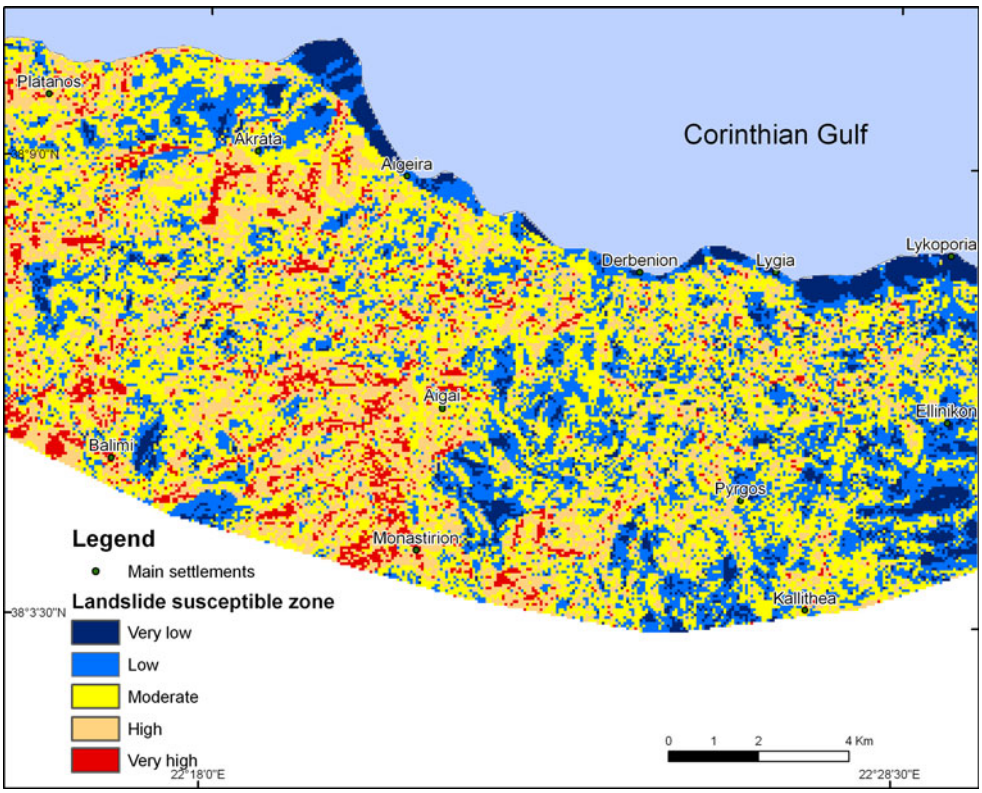

Fig. 7 The landslide susceptibility map from the AHP method

Table 5 Density percentages for landslide susceptibility zones for RES and AHP methods

Landslide susceptibility zones	Landslide density from the map of RES method, in %	Landslide density from the map of AHP method, in %
Very low	1.62	1.89
Low	14.20	17.12
Medium	39.09	39.31
High	34.29	32.67
Very high	10.80	9.02

Table 6 LaMI of very high susceptibility and high susceptibility zones from RES and AHP

	LaMI from the RES method	LaMI from the AHP method
Very high susceptibility zone	1.69	1.38
High susceptibility zone	1.37	1.32

Comparing the LAMI with the degree of fit (Irigaray 1995) which is calculating using the following equation:

$$\mathrm{DF} = \frac{z_i/S_i}{\sum \frac{z_i}{s_i}}$$

where z_i is the area affected by landslide in the i class of susceptibility, S_i is the area of this class of susceptibility (i) it was found that both validation procedures give exactly the same numerical results as their philosophy is matching.

Summing up the above discussion, it is revealed that RES method gives better results regarding the performance of the high and very high susceptibility zones (better concentration in prone to landslide areas, better LaMI values), mainly because of the binary interaction of the selected principal parameters. This interaction eliminates any subjective judgment of the experts and so, the resulting weighting coefficients express the maximum possible objectivity (Rozos et al. 2008).

Conclusions

The objective of this study was the comparison of two semi-quantitative methods, namely RES and AHP, which are among the effective tools of the experts for weighting and ranking parameters in a relatively simple way. This comparison was made taking into account the susceptibility zones, which were produced from the spatial distribution of landslides in eastern Achaia County. The study site was separated in two parts, the ranking area and the validating area. In the ranking area (with 277 recorded landslides) the

processing and the analysis of the data were made, while in the validating area (with 270 recorded landslides) a landslide susceptibility map was compiled and validated for both methods. Ten principal parameters subdivided in 5 classes with a rating from 0 to 4 were selected and applied in both methods and the weighting coefficients derived from the procedures of the methods, helped in the compilation of the final landslide susceptibility maps. GIS was engaged for the creation the layers of all the parameters involved, but also the two final maps for the landslide susceptibility zones. The comparison of these maps revealed that the RES method gives better results regarding the spatial distribution and the concentration of the most important susceptibility zones, i.e., depicting better the various zones in the most prone to landslide sites as its approximation helps in the elimination of any false judgment.

References

Akgün A, Bulut F (2007) GIS-based landslide susceptibility for Arsin-Yomra (Trabzon, North Turkey) region. Environ Geol 51:1348–1377. doi:10.1007/s00254-006-0435-6

Akgün A, Dag S, Bulut F (2008) Landslide susceptibility mapping for landslide-prone area (Findikli, NE Turkey) by likelihood-frequency ratio and weighted linear combination models. Environ Geol 54:1127–1143. doi:10.1007/s00254-007-0882-8

Ayalew L, Yamagishi H (2005) The application of GIS-based logistic regression for landslide susceptibility mapping in the Kakuda-Yahiko Mountains, Central Japan. Geomorphology 65:15–31

Ayalew L, Yamagishi H, Ugawa N (2004) Landslide susceptibility mapping using GIS-based weighted linear combination, the case in Tsugawa area of Agano River, Niigata Prefecture, Japan. Landslides 1:73–81. doi:10.1007/s10346-003-0006-9

Ayalew L, Yamagishi H, Marui H, Kanno T (2005) Landslides in Sado Island of Japan: Part II. GIS-based susceptibility mapping with comparisons of results from two methods and verifications. Eng Geol 81:432–445

Bathrellos GD, Kalivas DP, Skilodimou HD (2009) GIS-based landslide susceptibility mapping models applied to natural and urban planning in Trikala, Central Greece. Estud Geol 65:49–65. doi:10.3989/egeol.08642.036

Bossard M, Feranec J, Otahel J (2000) CORINE land cover technical guide—Addendum 2000. European Environment Agency, Copenhagen, p 104

Carrara A, Cardinali M, Detti R, Guzzetti F, Pasqui V, Reichenbach P (1991) GIS techniques and statistical models in evaluating landslide hazard. Earth Surf Proc Land 16:427–445

Casale R, Margottini C (1999) Floods and landslides. Springer, Berlin

Castellanos Abella EA, Van Westen CJ (2007) Generation of landslide risk index map for Cuba using spatial multi-criteria evaluation. Landslides 4:311–325. doi:10.1007/s10346-007-0087-y

Chau KT, Sze YL, Fung MK, Wong WY, Fong EL, Chan LCP (2004) Landslide hazard analysis for Hong Kong using landslide inventory and GIS. Comput Geosci 30:429–443

Donati L, Turrini MC (2002) An objective method to rank the importance of the factors predisposing to landslides with the GIS methodology: application to an area of the Apennines (Valnerina; Perugia, Italy). Eng Geol 63:277–289

Doutsos T, Kontopoulos N, Frydas D (1987) Neotectonic evolution of northwestern—continental Greece. Geol Rundsch 76:433–450

Doutsos T, Kontopoulos N, Poulimenos E (1988) The Corinth–Patras rift as the initial stage of continental fragmentation behind an active island arc (Greece). Basin Res 1/3:177–190. doi:10.1111/g.1365-2117.1988.tb00014.x

Gaki-Papanastassiou K, Papanastassiou D, Maroukian H (1996) Geomorphic and archaeological—historical evidence for past earthquakes in Greece. Ann Geofis 39:589–601

Glade T (1998) Establishing the magnitude and frequency of landslide triggering rainstorm events in New Zealand. Environ Geol 35:2–3

Guthrie RH, Evans SG (2004) Analysis of landslide frequencies and characteristics in a natural system, coastal British Columbia. Earth Surf Proc Land 29:1321–1339

Guzzetti F, Carrara A, Cardinali M, Reichenbach P (1999) Landslide hazard evaluation: a review of current techniques and their application in a multi-scale study, Central Italy. Geomorphology 31:181–216

Helias DI (1978) Some meteorological and climatological data of Rio-Antirio bridge site. In: Proceedings of international congress for Rio-Antirio bridge site. Editor University of Patras, Patra, pp 17–34

Hudson JA (1992) Rock engineering systems. Theory and practice, Ellis Horwood series in Civil Engineering, pp 185

IGME (1993) Geological map of Greece, at a scale of 1:50,000, Dervenion sheet, Athens

IGME (2005) Geological map of Greece, at a scale of 1:50,000, Aigion sheet, Athens

Irigaray C (1995) Movimientos de ladera: inventoria, analisis y cartografaa de susceptibilidad mediante un Sistema de Informacion Geografica. Aplicacion a las zonas de Colmenar (Ma), Rute (Co) y Montefrio (Gr). Thesis Doctoral, University Granada

Irigaray C, Fernandez T, El Hamdouni R, Chacon J (1999) Verification of landslide susceptibility mapping. A case study. Earth Surf Proc Land 24:537–544

Irigaray C, Fernandez T, El Hamdouni R, Chacon J (2007) Evaluation and validation of landslide-susceptibility obtained by GIS matrix method: examples from the Betic Cordillera (southern Spain). Nat Hazards 41:61–79

Jurko J, Paudits P, Vlcko J (2005) Landslide susceptibility zonation using GIS-statistical approach. In: International symposium on latest natural disasters—new challenges for engineering geology, IAEG, 1–7, September, Sofia

Kanungo DP, Arora MK, Sarkar S, Gupta RP (2006) A comparative study of conventional, ANN black box, fuzzy and combined neural and fuzzy weighting procedures for landslide susceptibility zonation in Darjeeling Himalayas. Eng Geol 85:347–366

Komac M (2006) A landslide susceptibility model using the analytical hierarchy process method and multivariate statistics in perialpine Slovenia. Geomorphology 74:17–28

Koukis G (1988) Slope deformation phenomena related to the engineering geological conditions in Greece. In: Proceedings of the 5th int symposium on landslides, vol 2, pp 1187–1192, Laussanne. Balkema, Rotterdam

Koukis G, Rozos D (1982) Geotechnical conditions and landslide phenomena in Greek territory, in relation with geological structure and geotectonic evolution. Mineral Wealth 16:53–69 (in Greek, with summary in English)

Koukis G, Sabatakakis N (2000) Engineering geological environment of Athens, Greece. Bull Eng Geol Environ 59:127–135

Koukis G, Rozos D, Hatzinakos I (1997) Relationship between rainfall and landslides in the formations of Achaia County, Greece. In: Proc of international symposium of IAEG in engineering geology and the environment, Balkema, Rotterdam, vol 1, pp 793–798

Lan HX, Zhou CH, Wang LJ, Zhang HY, Li RH (2004) Landslide hazard spatial analysis and prediction using GIS in the Xiaojiang watershed, Yunnan, China. Eng Geol 76:109–128

Larsen MC, Parks JE (1997) How wide is a road? The association of roads and mass movements in a forested montane environment. Earth Surf Proc Land 22:835–848

Lee S, Pradhan B (2007) Landslide hazard mapping at Selangor, Malaysia using frequency ratio and logistic regression models. Landslides 4:33–41. doi:10.1007/s10346-006-0047-y

Lee S, Sambath T (2006) Landslide susceptibility mapping in the Dammrei Romel area, Cambodia using frequency ratio and logistic regression models. Environ Geol 50:846–855

Mazzoccola DE, Hudson JA (1996) A comprehensive method of rock mass characterization for indicating natural slope instability. Q J Eng Geol 29:37–56

Moreiras SM (2005) Landslide susceptibility zonation in Rio Mendoza Valley, Argentina. Geomorphology 66:345–357

Papanastassiou D, Maroukian H, Gaki-Papanastassiou K (1993) Morphotectonic and archaeological observations in the eastern Argive plain (eastern Peloponnese, Greece) and their paleoseismological implications. Zeischrift Geomorphol 94:95–105

Parise M (2001) Landslide mapping techniques and their use in the assessment of the landslide hazard. Phys Chem Earth (C) 26:697–703

Remondo J, Gonzalez A, Diaz de Teran JR, Cendrero A, Fabbri A, Cheng CF (2003) Validation of landslide susceptibility maps: examples and applications from a case study in Northern Spain. Nat Hazards 30:437–449

Rozos D (1989) Engineering-geological conditions in the Achaia County. Geomechanical characteristics of the Plio-pleistocene sediments. PhD thesis, University of Patras, Patras, pp 453 (in Greek, with extensive summary in English)

Rozos D, Tsagaratos P, Markantonis K, Skias S (2006) An application of rock engineering system (RES) method for ranking the instability potential of natural slopes in Achaia County, Greece. In: Proc. of XIth international congress of the society for mathematical geology, University of Liege, Belgium, S08-10

Rozos D, Pyrgiotis L, Skias S, Tsagaratos P (2008) An implementation of rock engineering system for ranking the instability potential of natural slopes in Greek territory. An application in Karditsa County. Landslides 5:261–270. doi:10.1007/s10346-008-0117-4

Saaty TL (1977) A scaling method for priorities in hierarchical structures. J Math Psychol 15:234–281

Saaty TL (1990) How to make a decision: the analytic hierarchy process. Eur Oper Res 48:2–26

Saaty TL (2006) Rank from comparisons and from ratings in the analytic hierarchy/network processes. Eur Oper Res 168:557–570

Saha AK, Gupta RP, Arora MK (2002) GIS-based landslide hazard zonation in the Bhagirathi (Ganga) Valley, Himalayas. Int J Remote Sens 23:357–369

Skidmore M (2001) Risk, natural disasters, and household saving in life cycle model. Japan World econ 13:15–34

Tsoflias P (1970) Geological structure of the Northern part of Peloponnesus (Achaia County). Ann Geol d. Pays Hell. XXI:554–651, Athens

Van Westen CJ, Seijmonsbergen AC, Mantovani F (1999) Comparing landslide hazard maps. Nat Hazards 20:137–158

Yalcin A, Bulut F (2007) Landslide susceptibility mapping using GIS and digital photogrammetric techniques: a case study from Ardesen (NE-Turkey). Nat Hazards 41:201–226. doi:10.1007/s11069-006-9030-0

Yilmaz I (2009a) Landslide susceptibility mapping using frequency ratio, logistic regression, artificial neural networks and their comparison: a case study from Kat landslides (Tokat-Turkey). Comput Geosci 35:1125–1138

Yilmaz I (2009b) The effect of the sampling strategies on the landslide susceptibility mapping by conditional probability (cp) and artificial neural networks (ANN). Environmental Earth Sciences, Published online. doi:10.1007/s12665-009-0191-5

Yoshimatsu H, Abe S (2006) A review of landslide hazards in Japan and assessment of their susceptibility using analytical hierarchy process (AHP) method. Landslides 3:149–158. doi:10.1007/s10346-005-0031-y